Study of Planar Wideband mm-Wave Bowtie Antennas Over PCB Ground Plane

Marko Sonkki[1], Zeeshan Siddiqui[1], Jiangcheng Chen[1], Marko E. Leinonen[1], Markus Berg[1], Aarno Pärssinen[1]
[1] Centre for Wireless Communications, University of Oulu, Oulu, Finland, email: marko.sonkki@oulu.fi

***Abstract*—This paper presents a bowtie antenna structure integrated on PCB, where on the other side of the substrate is the antenna itself, and on the other side is a conductive ground plane. Three different cases are studied with simulations and measurements in terms of -10 dB impedance matching within 24-40 GHz bandwidth, depending on studied antenna structure. These three cases are linearly polarized single-ended bowtie, linearly polarized differentially fed bowtie, and differentially fed dual-polarized bowtie antenna. All antenna structures are on the ground plane of size 10 mm x 10 mm for easier comparison. Manufactured prototype antennas are measured and simulated with a 50 Ω coaxial feed. Simulated polarization properties and 3D radiation patterns of the dual-polarized bowtie are presented at 28 GHz and 34 GHz, which both shows 95% simulated total efficiency. Over the studied frequency range, the simulated total efficiency is better than 50%.**

***Index Terms*—antenna isolation, differential feed, dual linear polarization, mutual coupling, printed circuit board, single-ended feed,**

I. INTRODUCTION

Fifth-generation (5G) wireless communication systems are expected to provide 1000-fold high-speed wireless data transmission with low latency compared with the systems nowadays. A 5G wireless system offers a spectrum for higher data rates available for customer needs by using higher frequencies. A rapid development in radio tele-communications systems must meet these requirements in the future. Nowadays, the evolution of wireless access technologies are reaching these demands covering millimeter waves (mm-Wave) [1], where spectrum is highly attractive because of the available bandwidth [2][3].

In order to support multiple bands, especially for cellular applications, antennas with wide frequency range are preferred. Antennas should be not only easy to integrate with active and passive components but also fabricated by a simple manufacturing process. To integrate various wireless systems into a single device, components including antennas must be small to guarantee a compact integration and optimum functionality.

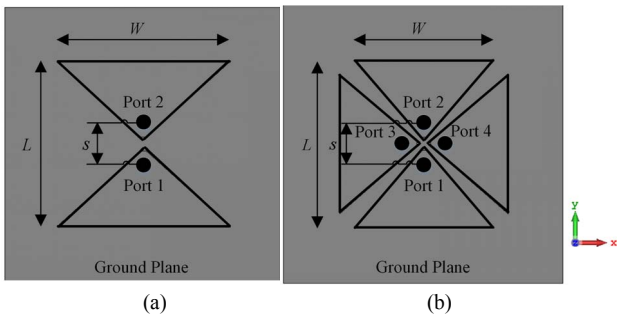

(a) (b)

Fig. 1. (a) Linear and (b) dual-polarized bowtie antenna structures with dimension variables and coordinate system. Gray color corresponds with conducting material.

Planar structures such as microstrip antennas are a flexible and cost-effective candidate for many applications. Planar dipoles and bowtie structures can be wideband [4][5] but with a dipole kind of structures a balun is needed to support a proper performance, corresponding to a differentially fed excitation. However, bowtie structures have been mostly designed for lower frequency bands with air between antenna and the reflector/ground plane [6]-[9]. In order to achieve the same performance at mm-waves, size restrictions need to be accounted, along with the low cost manufacturing methods.

The bow-tie-shaped antennas integrated on PCB (Printed Circuit Board) with ground plane are not intensively investigated for broadband application over the past years [10][11]. The reason for this might be that in theory, the optimum distance of a radiating element from a conducting reflector is defined as λ/4. Then, the reflection from the reflector is in-phase with the signal according to the direction of propagation.

This paper presents a simple bowtie antenna structure for mm-Waves designed to a two layer PCB. Below the bowtie antenna is the substrate layer, and below that, a conductive ground plane is applied. For authors' best knowledge, dual-polarized bowtie antenna structures at mm-Waves integrated on PCB has not been presented in the literature.

II. ANTENNA STRUCTURE

This section presents the studied bowtie antenna structure integrated on PCB and on a conductive ground plane. Fig. 1 presents linear and dual-polarized bowtie antenna structures with the dimension variables and coordinate system. The variables for different bowtie antenna scenarios is shown in Table I in terms of antenna width *W*, length *L*, feed point separation *s*, and characteristic impedance in Ω. The prototypes are made of the simulation models with coaxial feed, and the fabricated prototype antennas are presented in Fig. 2.

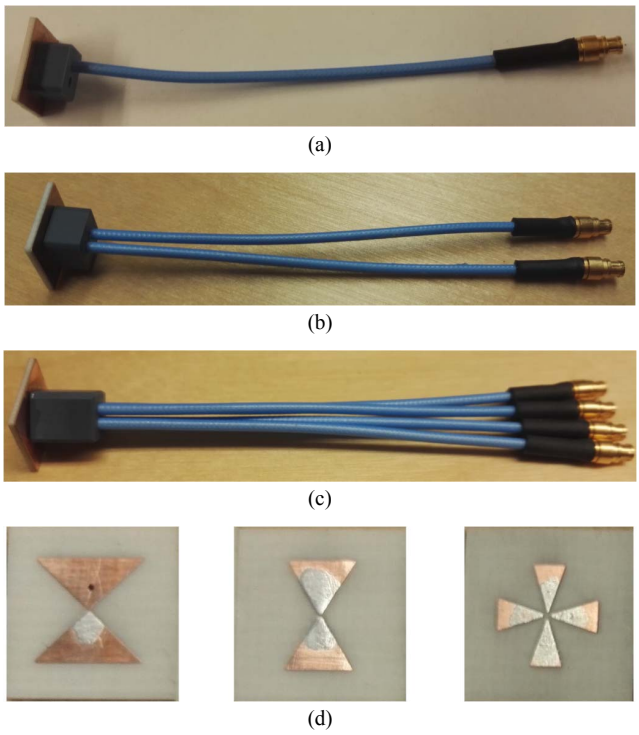

Fig. 2. Prototype of (a) singl-ended bowtie, (b) differentially fed bowtie, and (c) differentially fed dual-polarized bowtie antenna. (d) presents the prototype antennas in front view. The left one is linearly polarized single-ended bowtie, the middle is linearly polerized differentially fed bowtie, and the right one dual-polarized differentially fed bowtie.

The bowtie study is divided to two phases. First, linearly polarized antenna structures are investigated with single-ended and differentially fed cases to test the correlation between the simulations and measurements. In single-ended cases, the Port 2 is short-circuited. In the differential case, both ports are designed to the same impedance.

The single-ended and differential approaches are chosen as power amplifiers (PA) and/or low noise amplifiers (LNA) can be implemented either as single-ended or differential structures. The latter provides an opportunity to develop two times more power when transistor technology, like CMOS (Complementary Metal–Oxide–Semiconductor), will deliver limited power from a single transistor output stage.

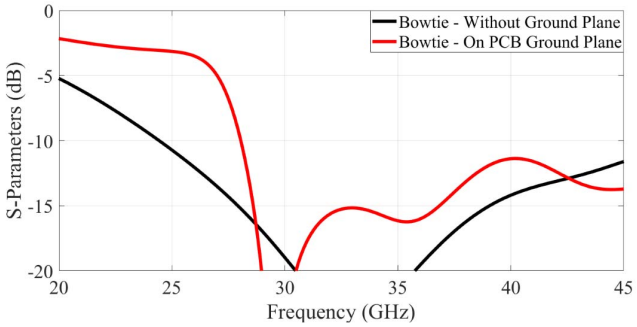

Fig. 3. Simulated frequency response of the bowtie antenna with and without ground plane. The ground plane is implemented on the opposite side of the subsrate as the bowtie antenna.

Secondly, after studying the linear polarization, the differentially fed antenna is extended to a dual-polarized antenna structure. S-parameters are measured and compared to the simulated ones in this case as well. A coaxial probe feed with waveguide port excitation is used to excite and measure the antenna S-parameters. CST Microwave Studio is used in the simulations.

In all the studied cases, the ground plane and substrate size is fixed to 10 mm x 10 mm. The used laminate is Rogers 4003C with 0.813 mm substrate thickness ($\varepsilon = 3.38$). In terms of wavelength, the electric distance of the bowtie antenna from the conductive ground plane is 0.12λ-0.20λ, depending on the frequency (24-40 GHz). Thus, in theory the optimum λ/4 distance with the used laminate electric properties is at 50 GHz. The effect of the size of the ground plane is not investigated in this study.

III. RESULTS

This section presents the simulated and measured results of the studied bowtie antenna cases defined in the Section II. First, linearly polarized bowtie is simulated with and without ground plane to understand the effect of the ground plane in a frequency domain and to the characteristic impedance. Then, simulated and measured results are studied in terms of impedance matching. Structures are studied in two cases: single-ended and differential. In single-ended case, the Port 2 is short-circuited (see Fig. 1(a)).

Then, the linearly polarized differentially fed approach is extended to a dual-polarized structure. The differential structure is chosen because it predicts better isolation between antenna ports and polarization [7], although feeding mechanism become more complex. The antenna performance is studied in terms of impedance matching and mutual coupling in terms of simulations and measurements. Finally, the simulated radiation properties of the dual-polarized structure is presented.

As the differentially fed antenna structures needs a balun, like a bowtie antenna, the measurements presented in this paper are performed by using Keysight PNA-X vector network analyzer (VNA). The Keysight PNA-X is 4-port VNA with differential measurement option.

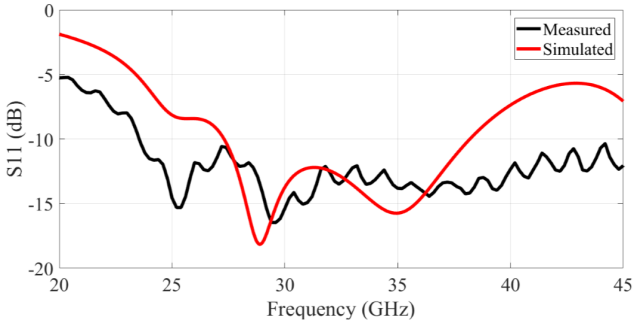

Fig. 4. Measured and simluated frequency response of the linearly polarized single-ended bowtie antenna with ground plane.

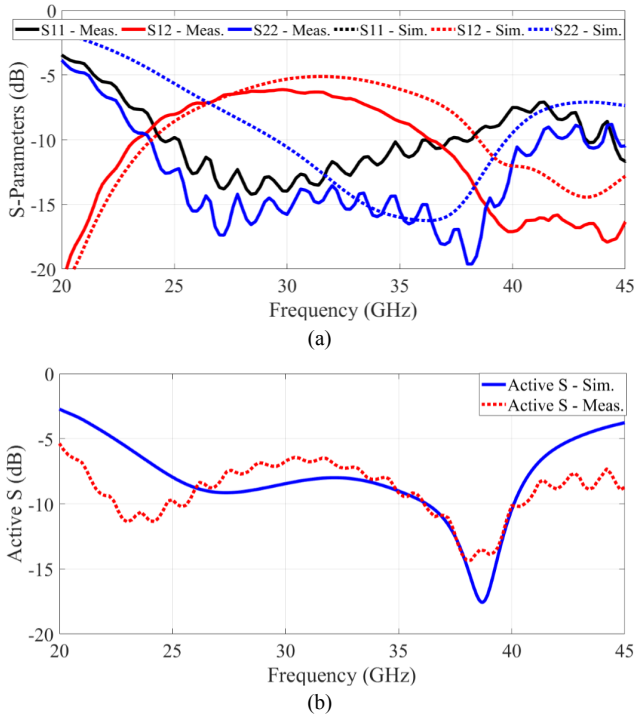

Fig. 5. Measured and simluated frequency response of the differentially fed linearly polarized bowtie antenna with ground plane. (a) S-parameters and (b) Active S-parameters (differential).

A. *Linearly Polarized Bowtie Antenna*

Fig. 3 presents simulated results of the bowtie antenna with and without ground plane. The simulations are done with a discrete port to find a characteristic impedance. The dimensions of the structures are presented in the Table I. As it can be observed, the bowtie without ground plane, the lower frequency start at 24 GHz when with the structure with ground plane, the lower frequency starts at 28 GHz. This appears because the bowtie with ground plane has strongly capacitive behavior below 28 GHz.

Fig. 4 presents the measured and simulated results of the single-ended bowtie antenna. The prototype antenna is shown in Fig. 2 (a) and (d). The simulated frequency response predicts -10 dB impedance bandwidth from 26 GHz to 38 GHz. The measured one shows -10 dB impedance bandwidth up from 24 GHz.

Fig. 5 presents measured and simulated frequency response of the differentially fed bowtie antenna. The prototype is shown in Fig. 2(b) and (d). Results are presented in terms of S-parameters and Active S-parameters. Active S-parameters corresponds here with the differential feeding where two port are excited with the same amplitude but in the opposite phase. As it can be observed, the simulated results well correlates with the measured ones. The simulated Active S-parameter frequency response predicts -8 dB impedance bandwidth from 25 GHz to 41 GHz, whereas the measured one presents slightly higher matching (-6 dB) with 21 GHz lower frequency limit.

As a conclusion of the studied linearly polarized bowtie antennas, the simulated results followed the measured with a fair margin. The ripple seen in the measurements are related to the cables in the prototype antennas, as they could not be calibrated out in this case. As going to higher frequencies, the accuracy of the simulation models and the manufacturing tolerances become more critical. As shown in [11], getting better than -10 dB impedance matching is challenging with differential structures.

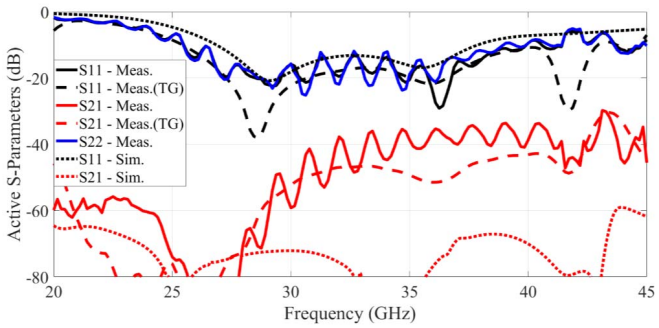

Fig. 6. Measured and simluated frequency response of the differentially fed dual-polarized bowtie antenna with ground plane. S11 = excitation of Port 1 and Port 2, S_{22} = excitation of Port 3 and Port 4, S_{21} = mutual coupling between the S_{11} and S_{22}., and (TG) equals to Time Gating.

B. *Dual-Polarized Bowtie Antenna*

As discussed earlier, the differentially fed structure is chosen for a dual-polarized structure because better isolation properties between the antenna ports. Fig. 6 presents the measured and simulated frequency response of the differentially fed dual-polarized bowtie antenna. The prototype antenna is shown in Fig. 2(c) and (d).

The simulated results predicts -10 dB impedance bandwidth from 27 GHz to 38 GHz, corresponding to 34% relative bandwidth. The correlation with the measured results is good even the measurements have quite much ripple caused by the cables as concluded in the case of linear polarization.

To calibrate out the ripple, The Hanning Time Gating (TG) window is used in the impulse response domain, which also set down the noise level by improving dynamics. By using the TG, the -10 dB impedance bandwidth slightly improves from 25.4 GHz to 40 GHz, corresponding to 45%

TABLE I. BOWTIE ANTENNA PARAMETERS

Bowtie	**Antenna Parameter**			
	***W* [mm]**	***L* [mm]**	***s* [mm]**	***Impedance* [Ω]**
	Linearly Polarized			
Without ground *Discrete port*	3.35	3.40	-	120
With ground *Discrete port*	6.25	6.00	-	115
Single-ended *Coaxial probe*	6.50	6.00	2.00	50
Differential *Coaxial probe*	4.00	6.25	1.95	50
	Dual-Polarized			
Dual-polarized *Discrete port*	6.3	6.6	-	80
Dual-polarized *Coaxial probe*	1.85	5.75	2.5	50

relative bandwidth.

What comes to the Active S_{21} between the two polarizations, the simulations are predicting better than 60 dB isolation, whereas the unfiltered measurements shows better than 35 dB isolation. This kind of measured result is expected closer to reality as the predicted coupling is very low. However, by using TG, the isolation is improved, and it is better than 43 dB.

It can be conclude here, besides concluded in the case of linear polarization, that the S_{21} parameter is extremely sensitive for the surroundings and calibration, as small variation in the measured phase causes large changes in the isolation.

C. *Simulated Radiation Properties of Dual-Polarized Bowtie*

Fig. 7 (a) presents the simulated Phi and Theta polarization components of the dual-polarized bowtie antenna at 28 GHz and 34 GHz. In the figure, P1 represents the balanced combination of Port 1 and Port 2, and P2 balanced combination of Port 3 and Port 4, respectively. As it can be observed, both polarizations are linearly polarized in both frequencies.

Fig. 7 (b) and (c) presents the simulated 3D radiation patterns of the dual-polarized bowtie antenna at 28 GHz and 34 GHz center frequencies. The maximum gain at the both presented frequencies is approximately 6 dBi. As it can be observed, at 34 GHz the directivity of the radiation pattern is not in the bore-sight anymore but in Theta = ±40°. This is caused by the currents in the ground plane, as the size become greater or equal to one lambda at the operating frequencies. Still, no deep zero is observed in boresight (Theta = 0°).

Fig. 7 (d) presents the simulated total efficiency of P1. The simulations predicts from -3 dB to -0.06 dB (50-98%) total efficiency over the 24-40 GHz operating bandwidth. The total efficiency of the presented radiation patterns at 28 GHz and 34 GHz is approximately -0.2 dB (95%).

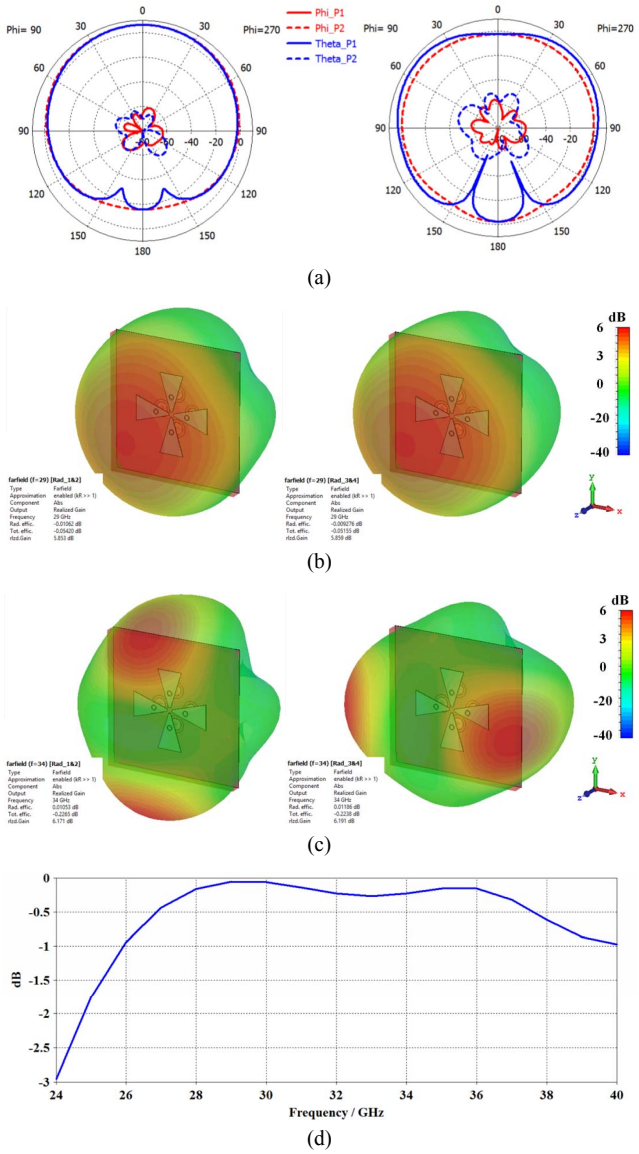

Fig. 7. (a) Simluated polarization components of dual-polarized differentially fed bowtie antenna at 28 GHz (left) and 34 GHz (right). The 3D radiation pattrens at (a) 28 GHz and (b) 34 GHz. The left side presents differential feed Active S_{11}, and the right side Active S_{22}. (d) Presents the simulated total efficiency of P1 as a function of frequency.

IV. CONCLUSIONS

The paper presented a linear and dual-polarized planar dipole structure implemented on the PCB. Three different cases were studied with simulations and measurements in terms of -10 dB impedance bandwidth. The results showed from 24 GHz to 40 GHz bandwidth, depending on the studied antenna structure. The studied three cases were linearly polarized single-ended bowtie, linearly polarized differentially fed bowtie, and differentially fed dual-polarized bowtie antenna.

All antenna structures were implemented on the ground plane of size 10 mm x 10 mm for fair comparison. Manufactured prototype antennas were measured and simulated with a 50 Ω coaxial feed. Simulated Phi and Theta polarization components as well as 3D radiation patterns of the dual-polarized bowtie were presented at 28 GHz and 34 GHz. Finally, the simulated total efficiency was presented over the studied frequency range, which predicted from -3 dB to -0.06 dB (50-98%) total efficiency.

ACKNOWLEDGMENT

This work has been funded by Business Finland project 5G Test Network Plus (5GTN+), and was partly supported by the Academy of Finland project 6Genesis Flagship (grant no. 318927).

REFERENCES

[1] T. Rappaport, et al. "Millimeter Wave Mobile Communications for 5G Cellular: It will work!.", *IEEE Access*, Vol. 1, 2013, pp. 335-349.

[2] Z. Pi and F. Khan, "An Introduction to Millimeter-Wave Mobile Roadband Systems", *IEEE Commuication. Magazine*, Vol. 49, No. 6, June 2011, pp. 101–107.

[3] A. I. Sulyman, A. T. Nassar, M. K. Samimi, G. R. Maccartney, T. S. Rappaport, and A. Alsanie, "Radio Propagation Path Loss Models for 5G Cellular Networks in the 28 GHz and 38 GHz Millimeter-Wave Bands", IEEE Communication Magazine, Vol. 52, No. 9, September 2014, pp. 78–86.

[4] J. Yang and A. Kishk, "A Novel Low-Profile Compact Directional Ultra-Wideband Antenna: the Self-Grounded Bow-Tie Antenna", *IEEE Transactions on Antennas and Propagation*, Vol. 60, No. 3, March 2012, pp. 1214–1220.

[5] H. Raza, A. Hussain, J. Yang, and P.-S. Kildal, "Wideband Compact 4-Port Ddual Polarized Self-Grounded Bowtie Antenna", *IEEE Transactionson Antennas and Propagation*, vol. 62, no. 9, September 2014, pp. 4468–4473

[6] Z. Yang, C. Zhang, Y. Yin, and Y. Wang, "A Wideband Dual-Polarized Modified Bowtie Antenna for 2G/3G/LTE Base-Station Applications", *Progress In Electromagnetics Research Letters*, Vol. 61, 2016, pp. 131–137.

[7] S.□G. Zhou, Z.□H. Peng, C.□Y.□D. Sim, "A Low□Profile, Dual□Polarized, and Wideband Square Cavity□Backed Antenna", *Wiley's International Journal of RF and Microwave Computer-Aided Engineering*, Vol. 28, Iss. 8, October 2016, pp. 724-730.

[8] M. Li, and K.-M. Luk, "Wideband Magnetoelectric Dipole Antennas With Dual Polarization and Circular Polarization", *IEEE Antennas and Propagation Magazine*, Vol. 57, Iss. 1, February 2015, pp. 110-119.

[9] Z.-Y. Zhang, S. Zuo, Y. Zhao, L.-Y. Ji, G. Fu, "Broadband Circularly Polarized Bowtie Antenna Array Using Sequentially Rotated Technique", *IEEE Access*, Vol. 6, Feb. 2018, pp. 12769-12774.

[10] S. Mukherjee, A. Biswas, and K. V. Srivastava, "Broadband Substrate Integrated Waveguide Cavity-Backed Bow-Tie Slot Antenna", *IEEE Antennas and Wireless Propagation Letters*, Vol. 13, June 2014, pp. 1152-1155.

[11] S. M. Moghaddam, J. Yang, A. A. Glazunov, "Ultra-Wideband Millimeter-Wave Bowtie Antenna", *International Symposium on Antennas and Propagation (ISAP)*, 30th Oct.-2nd Nov. 2017.